The variability of the proton cosmic ray flux in and outside spiral arms. First results from calculations over long propagation times

Ingo Büsching*†, Marius S. Potgieter*†

*Unit for Space Physics, North-West University, 2520 Potchefstroom, South Africa
†The Centre for High Performance Computing, CSIR Campus, Rosebank, Cape Town, South Africa

Abstract. **Supernovae (SN) are the most likely sources of galactic cosmic rays. Since the most frequent SN types Ib and II are found within spiral arms, one can expect a significant difference in the range of possible spectra inside and outside spiral arms. We investigate the variability of the local interstellar cosmic ray proton spectrum during the motion of the Sun in and out of spiral arms along its journey around the galactic center. For this we calculated the cosmic ray density over a period of 100 Myr to allow for one spiral crossing at a given point at the galactocentric distance of the Sun.**

***Keywords*: Cosmic Rays, Galaxy, Spiral Arms**

I. Introduction

The discovery of direct evidence for high-energy particle acceleration in the shell of a supernova remnant (SNR) [1], [2] underlined the need to investigate the distribution of galactic cosmic rays (CR) on scales small enough to resolve the changes (spatial and temporal) in the CR density due to these kind of objects.

It has been shown earlier [5] that the discrete nature (both in space and time) of supernovae (SN), as sources of galactic CR leads to CR fluxes and spectra that change in space and time.

Taking into account that the most frequent SN types Ib and II are found within spiral arms [7], it was further found that the CR proton flux in the inter arm regions is less than inside the spiral arms [4].

In this work, we extend this study calculating the temporal evolution of the CR proton density over a time span of 100 Myr to allow for convergence of the CR proton density, taking into account the movement of the galactic spiral arms.

II. Galactic structure and Distribution of Cosmic Ray Sources

As pointed out by [7], the most frequent SN types Ib and II tend to cluster in spiral arms. Modelling the distribution of CR in the Galaxy, assuming the majority of CR is accelerated in SN, the spiral structure of the Galaxy has to be taken into account. Following [4], we calculate the evolution of the CR density distribution over a ten times larger time interval of 100 Myr. Over this time span, the motion of the galactic spiral arms, which in our model harbour the CR sources, can no longer be neglected. Following [9], [10], we assume that the spiral structure rotates around the galactic center with the pattern speed $\Omega_{\rm pattern}$. Shaviv [13] gives an overview of the pattern speed $\Omega_{\rm pattern}$ derived by various authors. Depending on the method used, the pattern speed is found to be in the range 10–30 (km/s)/kpc. We adopt $\Omega_{\rm pattern}$ = 16.9 (km/s)/kpc, the value found by [13] from HI observations.

We note the finding of [3] that the absence of an anisotropy in the CR flux due to the Sun's movement around the galactic center implies that the CR corotate with the local galactic magnetic environment. Calculating the evolution of the CR density in the frame of the local galactic magnetic environment, the spiral pattern speed with respect to this frame of reference is $\Omega\prime_{\rm pattern} \approx \Omega_{\rm sun} - \Omega_{\rm pattern}$. In this case, our adopted value of $\Omega_{\rm pattern}$ is just above the upper bound of the range for $\Omega\prime_{\rm pattern}$ as given in [13] and our calculations give a lower limit on the changes in the galactic CR distribution due to spiral arm movements.

III. The Model

The propagation of galactic CR protons in the diffusion picture taking into account energy and catastrophic losses is described by

$$\frac{\partial N}{\partial t} - S \quad = \quad k(p)\Delta N - \frac{\partial}{\partial p}\left(bN\right) - \Omega(z)\frac{N}{T}, \quad (1)$$

where N is the CR density, B the rate of momentum loss and T the time-scale of catastrophic losses. For the spatial diffusion coefficient $k(p)$, we assume an energy dependence in the form of a broken power law in rigidity, as suggested by the Boron to Carbon ratio

$$k(p) \quad = \quad \begin{cases} k_0\left(\zeta/\zeta_0\right)^{0.6} & \text{for } \zeta > \zeta_0 \\ k_0\left(\zeta/\zeta_0\right)^{-0.48} & \text{for } \zeta < \zeta_0 \end{cases} . \quad (2)$$

The current version of our code is not capable of dealing with momentum losses. We thus approximate them by catastrophic losses

$$T_{\rm cont}(p) \quad = \quad \frac{p}{b}, \quad (3)$$

where we used for b a fit from a Monte Carlo model, as given by [11].

For the source term S we assume stochastic SN events, modeled as point sources with a linear increase and an exponential cut-off for the CR acceleration. For the distribution of the SN events, we assume that the cluster in the galactic spiral arms, which rotate with a pattern speed $\Omega_{\rm pattern}$.

Considering the geometry of our Galaxy, a diffusive volume in the form of a cylinder with radius $R = 15$ kpc and height $2H$, with the Galactic disc in the mid-plane perpendicular to the the cylinder-axis is assumed. Thus the use of cylindrical coordinates is appropriate. The Laplacian in these coordinates is given as

$$\Delta N = \frac{1}{r}\frac{\partial N}{\partial r} + \frac{\partial^2 N}{\partial r^2} + \frac{1}{r^2}\frac{\partial^2 N}{\partial \varphi^2} + \frac{\partial^2 N}{\partial z^2}. \quad (4)$$

Eq. 1 with the Laplacian given by Eq. 4 is transformed by the ansatz

$$N = \frac{1}{\pi}\sum_n\sum_m \frac{\jmath_n(\alpha_{nm} r)}{(\jmath_n'(\alpha_{nm} R))^2} \times (A_{nm}\cdot\cos(n\varphi) + B_{nm}\cdot\sin(n\varphi)) \quad (5)$$

in a series of PDEs with one spatial dimension for the coefficients A_{nm}, B_{nm}. These are solved numerically using a Crank Nicholson scheme (see [5] for a full description of the method).

IV. Calculations

For our calculation of the evolution of the distribution of the CR proton component, we adopt the parameters $k_0 = 0.073\,\mathrm{kpc^2 Myr^{-1}}$, ζ_0=3 GV and H=4 kpc as given by [12] for their model without reacceleration. Note that while [12] used a gas distribution based on measurements, we assume a gas distribution varying only perpendicular to the galactic disk. We calculate the evolution of the CR proton distribution for a time span of 100 Myr and a total of 1300000 transient point sources clustering in spiral arms, starting with an empty Galaxy.

The total number of SN events was chosen to reproduce the observed local SN rate of $20\,\mathrm{Myr^{-1}kpc^{-2}}$ [8], while assuming a radial distribution as given by [6] (for a galactocentric distance of the Sun of 8.5 kpc) rescaled to a galactocentric distance of the Sun of 7.2 kpc as adopted in the model of the spiral structure.

We use the geometry for the galactic spiral arms as given by [15], with the arm width obtained by [14] for the free electron distribution, as the envelop of stochastic distributed CR sources. We further assume that the Galactic spiral structure rotates with the pattern speed $\Omega_{\mathrm{pattern}}$=16.9 (km/s)/kpc. The radial source distribution is taken from [6] and rescaled to the galactocentric distance of the spiral arm model.

For the calculation presented here, we considered 630×420 coefficients A_{nm}, B_{nm} of the double sum in Eq. (5), which yields a resolution of 75 pc in Galactocentric radius r and azimuth φ at the position of the Sun. The numerical grid used in z direction (perpendicular to the galactic plane) has a step size of 40 pc, the time step is 10 kyr (internal, a time step of 100 yr was used to guarantee numerical stability).

The computations were performed at the Centre For High Performance Computing, Meraka Institute, CSIR Rosebank, Cape Town.

V. Results

Results of our calculations are presented in Figs. 1, 2, 3. In Figures 1, 2, we show the temporal evolution of the CR proton density at the galactocentric distance of the Sun for particle energies of 5 GeV and 500 GeV and for two different points in the Galaxy (both at the galactocentric radius of the Sun). As can be seen in Figs. 1,2, while for 500 GeV protons, the inter-arm region fills up quite quickly, for 5 GeV protons it takes until the first spiral arm crossing to fill the region up the saturation level. In both cases, a CR level slightly lower than the base-line during the spiral arm crossing is maintained after the spiral arm moved over the region.

In Fig. 3, we show the range of possible spectra during a spiral arm crossing and in the inter arm region. These results are qualitatively similar to those obtained earlier [4] for calculations over the much shorter time span of 10 Myr starting from a steady state distribution of CR protons and neglecting the movement of the spiral arms.

VI. Summary and conclusion

We present first results of calculations of the distribution of CR proton component over a time span of 100 Myr, taking into account the rotation of the spiral arm pattern. The results we get for the range of possible spectra during a spiral arm crossing and in the inter arm region (after the passage of a spiral arm) are qualitatively similar to results obtained by [4] for calculations over 10 Myr starting from a steady state distribution of CR protons and neglecting the movement of the spiral arms.

We conclude that, at least for the parameters used in this study, it is permissible to start the calculations from a steady state distribution and neglect the movement of the spiral arms (i.e. the approach used in [4]) if one is interested in the influence of the spiral structure on the evolution and distribution of CR in the galactic disk.

References

[1] Aharonian, F., et al., (H.E.S.S. collaboration), *A detailed spectral and morphological study of the gamma-ray supernova remnant RX J1713.7-3946 with HESS*. A&A 449, 223 (2006)

[2] Aharonian, F., et al., (H.E.S.S. collaboration), *High energy particle acceleration in the shell of a supernova remnant* Nature 432, 75 (2004)

[3] Amenomori, A., et al., *Anisotropy and Corotation of Galactic Cosmic Rays* Science 314, 439 (2006)

[4] Büsching, I., Potgieter, M. S., *The variability of the proton cosmic ray flux on the Suns way around the galactic center* Advances in Space Research 42, 504 (2008)

[5] Büsching, I., et al., *Cosmic-Ray Propagation Properties for an Origin in Supernova Remnants*. ApJ 619, 314 (2005)

[6] Case, G., Bhattacharya, D., *Revisiting the galactic supernova remnant distribution.* A&AS 120, C437 (1996)

[7] Dragicevich, P. M., Blair, D. G., Burman, R. R., *Why are supernovae in our Galaxy so frequent?* MNRAS 302, 693 (1999)

[8] Grenier, I. A., *Gamma-ray sources as relics of recent supernovae in the nearby Gould Belt*. A&A 364, L93 (2000)

[9] C. C. Lin, F. H. Shu, *On the Spiral Structure of Disk Galaxies*. ApJ 140, 646 (1964)

[10] C. C. Lin, C. Yuan, F. H. Shu, *On the Spiral Structure of Disk Galaxies. III. Comparison with Observations*. ApJ 155, 721 (1969)

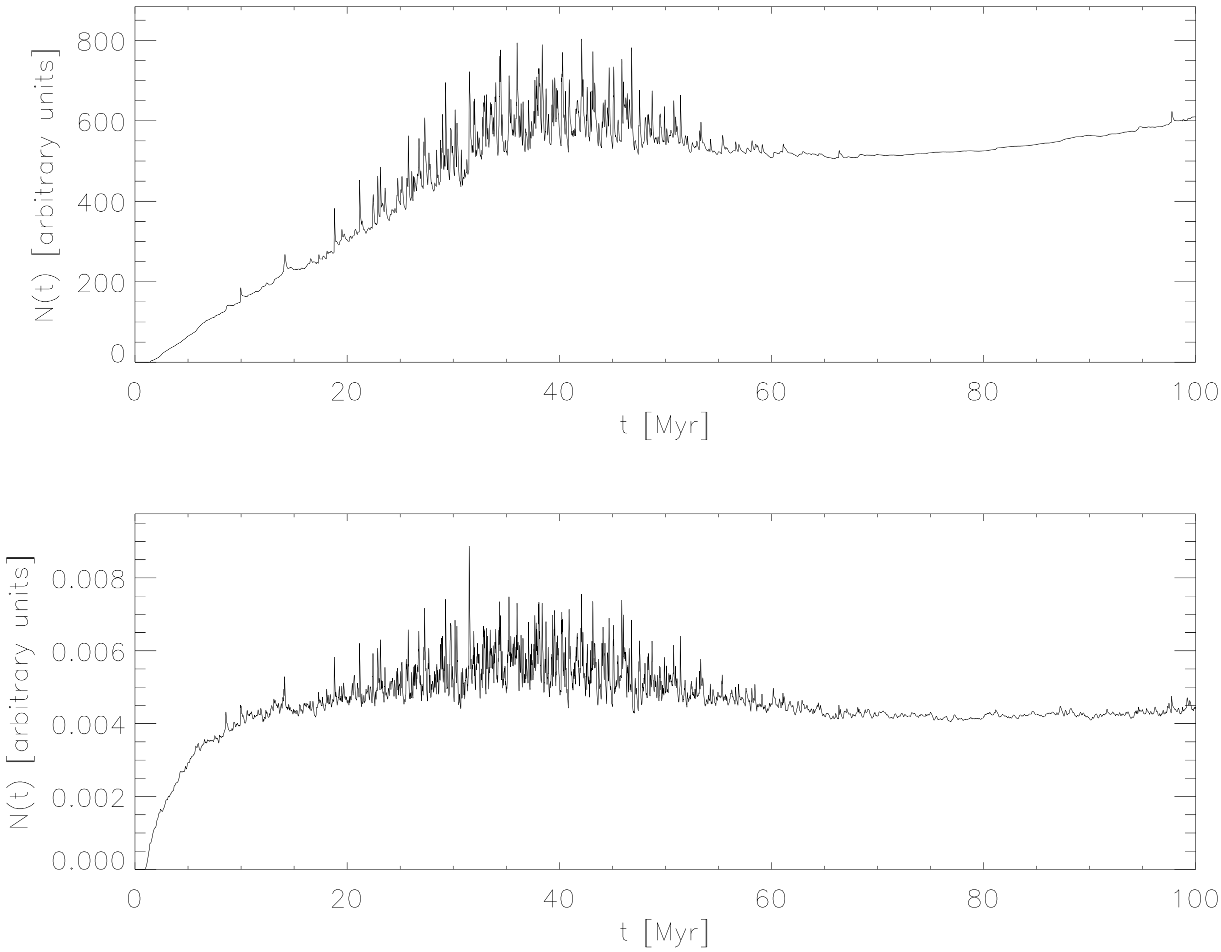

Fig. 1. Temporal variation of the CR proton flux at 5 GeV (upper panel) and 500 GeV (lower panel) at the galactocentric radius of the Sun. The passing of the spiral arm is clearly visible.

[11] Pohl, M., Schlickeiser, R., *On the conversion of blast wave energy into radiation in active galactic nuclei and gamma-ray bursts*. A&A 354, 395 (2000)

[12] Ptuskin, V. S., et al., *Dissipation of Magnetohydrodynamic Waves on Energetic Particles: Impact on Interstellar Turbulence and Cosmic-Ray Transport*. ApJ 642, 902 (2006)

[13] Shaviv, N. J., *The spiral structure of the Milky Way, cosmic rays, and ice age epochs on Earth*. New Astronomy 8, 39 (2003)

[14] Taylor, J. H, Cordes, J. M., *Pulsar distances and the galactic distribution of free electrons*. ApJ 411, 674 (1993)

[15] Vallée, J. P., *Metastudy of the Spiral Structure of Our Home Galaxy*. ApJ 566, 261 (2002)

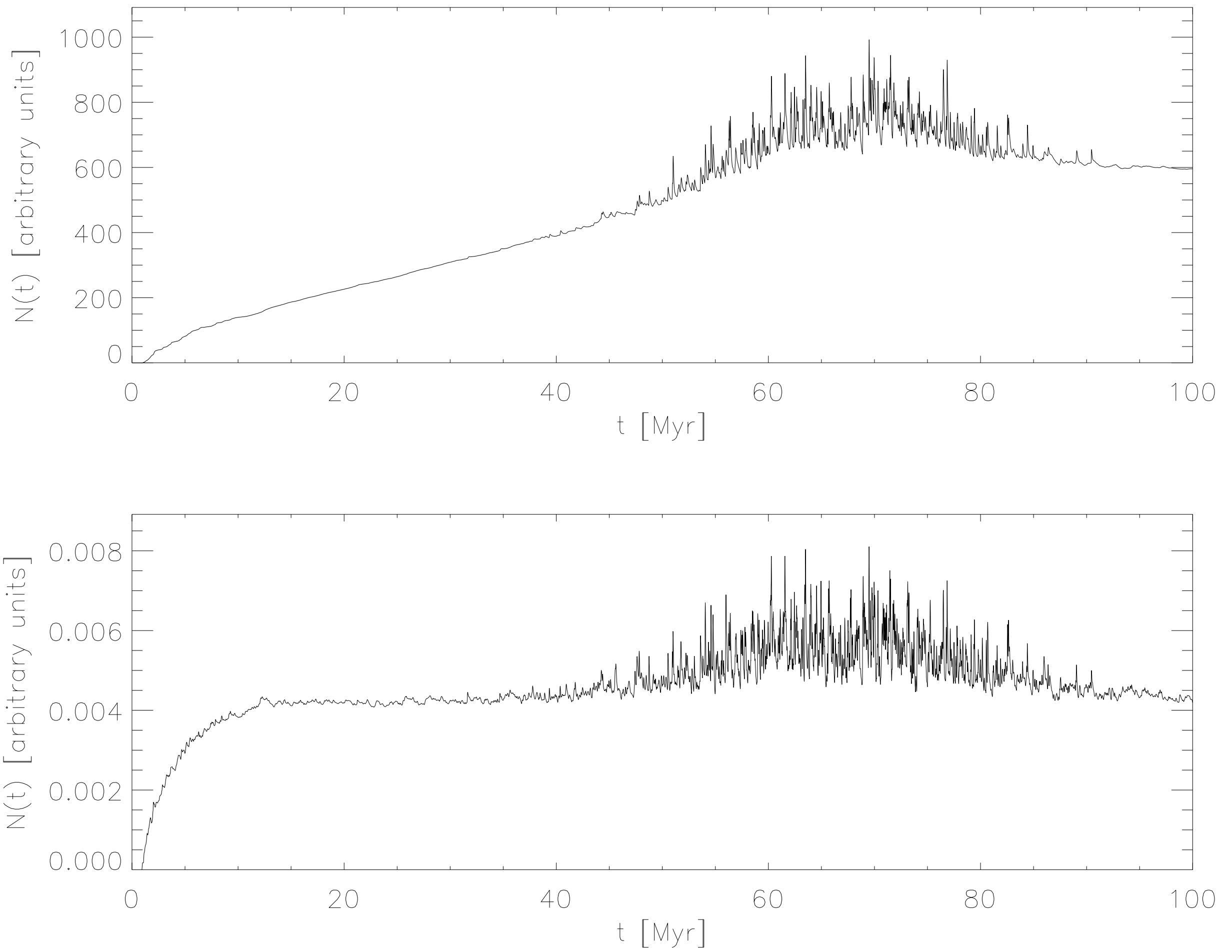

Fig. 2. Similar Fig. 1, but for a point in the galactic disc that was passed by a spiral arm at a later time.

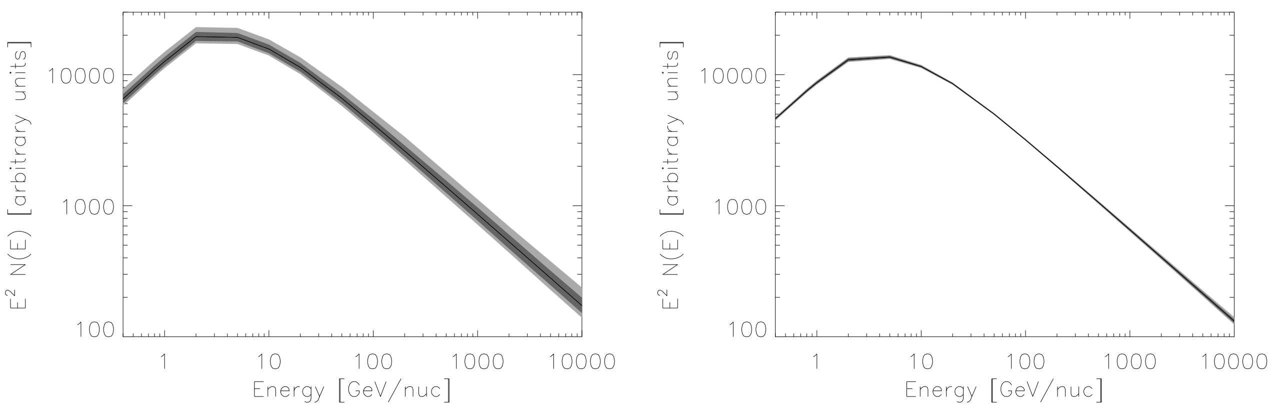

Fig. 3. Range of possible proton spectra during a spiral arm passage (left panel) and between spiral arm passages (right panel). The light grey band shows the range, where 95% of the possible spectra are located, the dark grey band gives the 68% range. The solid line marks the averaged spectrum.